

LIMIT CYCLES OF QUADRATIC SYSTEMS IN THE PLANE

L. M. PERKO

1. Introduction. This paper presents a study of the known limit cycle configurations for quadratic systems in the plane:

$$(1) \quad \begin{aligned} \dot{x} &= \sum_{i+j=1}^2 a_{ij}x^i y^j \\ \dot{y} &= \sum_{i+j=1}^2 b_{ij}x^i y^j. \end{aligned}$$

Concrete examples of quadratic systems with the following limit cycle configurations are known.

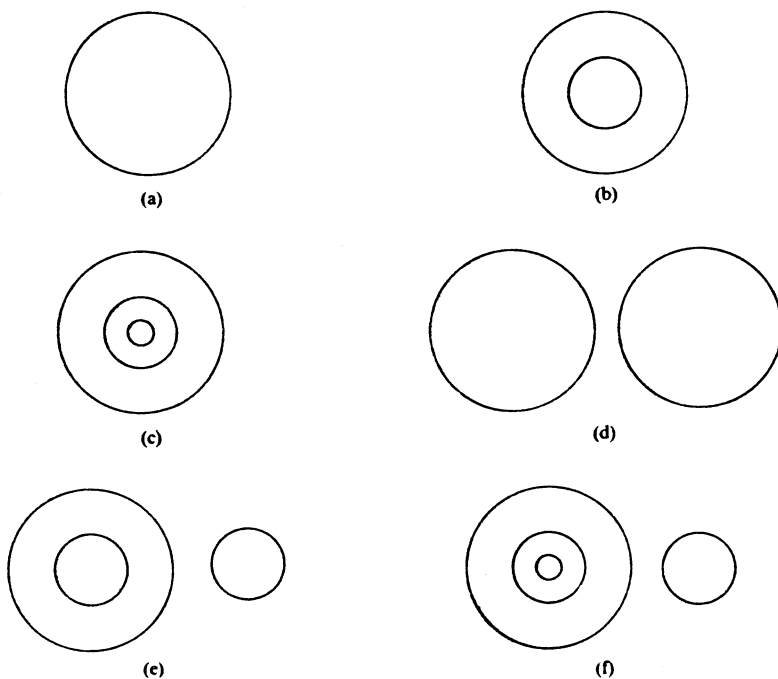


Figure 1

Received by the editors on August 12, 1983, and in revised form on September 26, 1983.

This work was supported by the National Science Foundation under Grant No. MCS-8201020.

Examples of the configuration (a) were given by Frommer [6] and Yeh Yen-chien [13]; the latter reference also includes a uniqueness proof. Examples of the configurations (b) and (c) were given by Bautin [2] and Chin [4]. They established that there are quadratic systems with two and three limit cycles in a small neighborhood of the origin; however, nothing is said about whether or not there are limit cycles outside of this small neighborhood of the origin. Examples of the configuration (d) were given by Yeh Yen-chien [12], Tung Chin-chu [11], and Perko [8]; however, the fact that there are exactly two limit cycles in the configuration (d) was only established in [8]. Tung Chin-chu [11] gave an example with at least three limit cycles in the configuration (e). And Shi Songling [10] gave an example with at least four limit cycles in the configuration (f), thereby disproving the assertion of Petrovskii and Landis [9] that a quadratic system can have at most three limit cycles. These examples represent all of the known limit cycle configurations for quadratic systems in the plane.

It was suggested by Chicone and Jinguang [3] that numerical plots be made for examples of quadratic systems exhibiting all of the known limit cycle configurations shown in Figure 1; cf. Problem 2.11, p. 172 in [3]. Computer plots for the limit cycle configurations (a) and (d) with exactly one and two limit cycles respectively were given in [8]. But computer plots have not been obtained for any of the other configurations in Figure 1.

Tung Chin-chu [11] gave an example of a quadratic system with three limit cycles in the configuration (e) of Figure 1; cf. Ex. 3, p. 170 in [11]. Tung's system forms a family of rotated vector fields with parameter α , and what Tung shows in [11] is that his system on p. 170 has at least three limit cycles in the configuration (e) for α small and negative. In §3 of this paper Duff's theory for limit cycles of rotated vector fields [5] and the extension in [7] are used to show that Tung's system has at least three limit cycles in the configuration (e) for all $\alpha \in (\alpha^*, 0)$ where α^* is determined numerically to be approximately equal to $-.0093$. The theory of rotated vector fields and the Poincaré-Bendixson Theorem are then used to determine the global behavior of the limit cycles of Tung's system as the vector field goes through one complete rotation; i.e., as α varies in $[-\pi, \pi)$. A computer plot of the three limit cycles in the configuration (e) of Figure 1 for Tung's system with a particular value of $\alpha \in (\alpha^*, 0)$ is also given in §3.

It is difficult if not impossible to obtain numerical plots of the limit cycles of Chin's examples in [4] exhibiting the configurations (b) and (c) and of the limit cycles of Songling's example in [10] exhibiting the configuration (f) because of the extremely small size of the coefficients and limit cycles in these examples. However, in §5 of this paper, the theory of rotated vector fields [5, 7] and some numerical experimentation is used to

modify Songling's example in order to obtain a quadratic system with four "normal-size" limit cycles in the configuration (f) of Figure 1. In fact, the numerical results in §5 of this paper strongly indicate that the quadratic system

$$\begin{aligned}\dot{x} &= P(x, y)\cos \alpha - Q(x, y)\sin \alpha \\ \dot{y} &= P(x, y)\sin \alpha + Q(x, y)\cos \alpha\end{aligned}$$

with

$$\begin{aligned}P(x, y) &= \lambda x - y - 10x^2 + (5 + \delta)xy + y^2, \\ Q(x, y) &= x + x^2 + (8\epsilon - 25 - 9\delta)xy,\end{aligned}$$

and $\alpha = -.0023$, $\lambda = -.005$, $\epsilon = -.01$, and $\delta = -.5$ has exactly four limit cycles in the configuration (f) of Figure 1. A numerical plot of these four limit cycles is given in §5. The same technique used to modify Songling's example could also be used to modify Chin's examples in order to obtain quadratic systems with "normal-size" limit cycles in the configurations (b) and (c) in Figure 1; however, this is not done in this paper. On the other hand, Mieussens [14] has obtained a modification of Chin's example with two "normal-size" limit cycles in the configuration (b) of Figure 1 and numerical plots of these limit cycles are given in §6 of this paper.

Thus, this paper surveys and adds a bit to the knowledge of limit cycle configurations of quadratic systems in the plane, and in particular it contains numerical plots of all of the known limit cycle configurations except the configuration (c) shown in Figure 1.

The recent survey paper of Chicone and Jinghuang [3] nicely summarizes the important facts known about quadratic systems in the plane; §2 on limit cycles is particularly relevant to this paper. And several facts about quadratic systems used in this paper, such as the conditions necessary and sufficient for a critical point to be a center, can be found in this survey paper.

The main analytical tool that is used to study the limit cycles of (1) in this paper is the theory for limit cycles of a family of rotated vector fields. A vector field is said to belong to a family of rotated vector fields with parameter $\alpha \in (a, b)$ if each vector in the vector field rotates through a positive angle as α increases in (a, b) . Any vector field, such as the vector field $\dot{x} = P(x, y)$, $\dot{y} = Q(x, y)$ defined by (1), can be embedded in a family of rotated vector fields with parameter $\alpha \in (-\pi, \pi)$ by setting

$$(1_\alpha) \quad \begin{aligned}\dot{x} &= P(x, y)\cos \alpha - Q(x, y)\sin \alpha \\ \dot{y} &= P(x, y)\sin \alpha + Q(x, y)\cos \alpha.\end{aligned}$$

In his theory for limit cycles of a family of rotated vector fields, [5], Duff

showed that a unique limit cycle is generated at the origin of (1_α) , with the determinant of the linear terms $a_{10}b_{01} - b_{10}a_{01} \neq 0$, at that value of α where the trace of the linear part, $\tau(\alpha) \equiv (a_{10} + b_{01})\cos \alpha + (a_{01} - b_{10})\sin \alpha$, vanishes provided that the origin is not a center at this value of α . Furthermore, he showed that this limit cycle expands monotonically with monotonically varying α , covering a deleted neighborhood of the origin until it either (i) intersects one or more critical points of (1_α) and forms a separatrix cycle, or (ii) intersects a second limit cycle of (1_α) and forms a semi-stable limit cycle, or (iii) becomes unbounded. The behavior of stable (-) and unstable (+) limit cycles of a family of rotated vector fields is summarized in the following table, given on p. 21 in [5]:

Orientation	+	+	-	-
Stability	-	+	-	+
Motion as $\alpha \uparrow$	Contracts	Expands	Expands	Contracts

These facts concerning limit cycles of families of rotated vector fields contained in [5], and several points of information about quadratic systems in the plane contained in the survey paper [3] will be used extensively throughout this paper.

2. Examples of the configurations (a) and (d).

It was established in [8] that for $0 < \alpha < 1$, the quadratic system

$$(2) \quad \begin{aligned} \dot{x} &= y + y^2 \\ \dot{y} &= -x + \alpha y - xy + (1 + \alpha)y^2 \end{aligned}$$

has exactly one limit cycle around the origin which is generated at $\alpha = 0$ and which expands monotonically to infinity as α increases to a value $\alpha^* \geq 1$. There are no limit cycles for $\alpha \leq 0$ and if $\alpha^* = 1$ the separatrix configuration for $-3 < \alpha \leq 1$ is given by

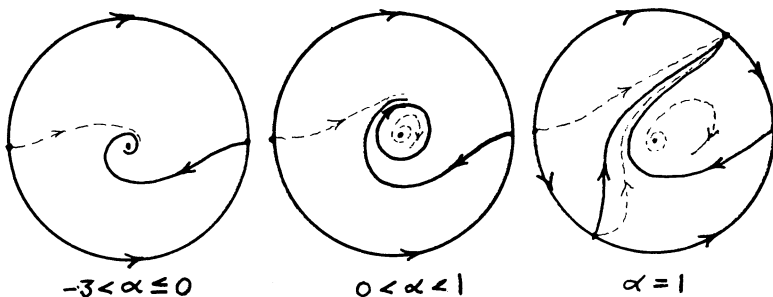


Figure 2

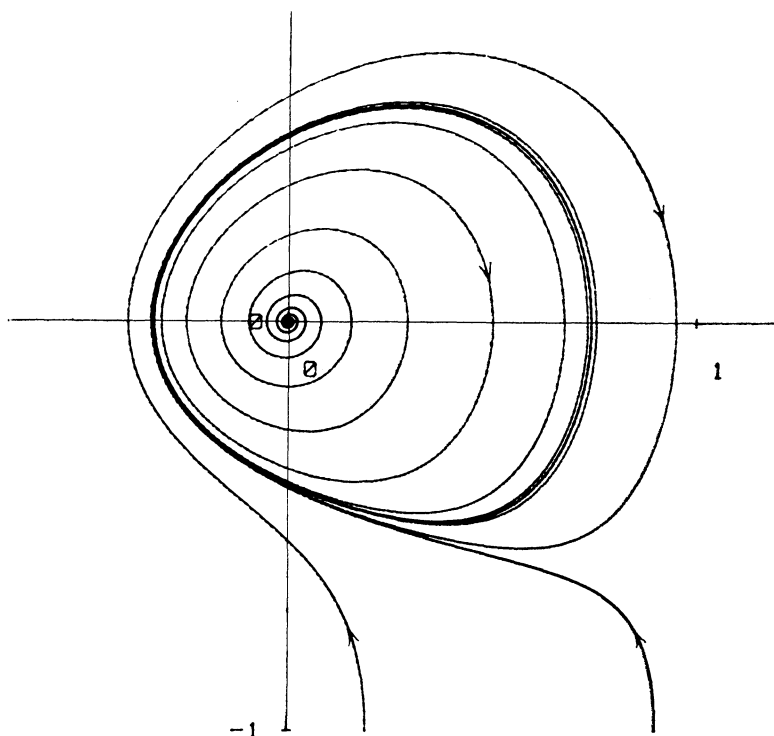


Figure 3

A computer plot for the system (2) with $\alpha = .2$ which clearly shows the stable, negatively oriented limit cycle for this system is given in Figure 3 above.

It was also established in [8] that for $0 < \alpha < .8$ the quadratic system

$$(3) \quad \begin{aligned} \dot{x} &= y + y^2 \\ \dot{y} &= -.5x + \alpha y - xy + (.8 + \alpha)y^2 \end{aligned}$$

has exactly one limit cycle around the origin and exactly one limit cycle around the critical point $(-1.6, -1)$; these limit cycles are generated at $\alpha = 0$ and they expand monotonically as α increases in the interval $(0, .8)$; they intersect in the line $y = -1/2$ at $\alpha = .8$; there are no limit cycles for $\alpha \leq 0$ or for $\alpha \geq .8$; and the separatrix configurations for $-2.8 < \alpha < 1.2$ are given in Figure 4 below.

A computer plot for the system (3) with $\alpha = .2$ showing the two limit cycles of this system is given in Figure 5 below.

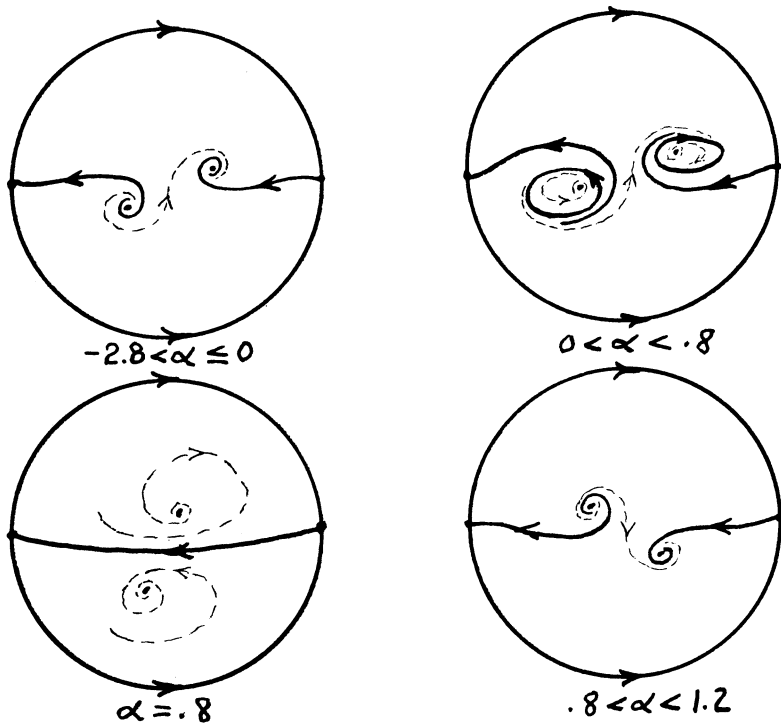


Figure 4

3. Tung Chin-chu's example of the configuration (e). It was established in [11] that for $-1 \ll \alpha < 0$ the quadratic system

$$(4) \quad \begin{aligned} \dot{x} &= P(x, y)\cos \alpha - Q(x, y)\sin \alpha \\ \dot{y} &= P(x, y)\sin \alpha + Q(x, y)\cos \alpha \end{aligned}$$

with $P(x, y) = xy$ and $Q(x, y) = -(1/3)(x - 1)(x + 2) + (1/2)y^2 + (1/3)xy - (1/3)y$ has at least three limit cycles in the configuration (e). The numerical results of this study indicate that this system has exactly three limit cycles in the configuration (e), but this still remains to be proved; cf. Problem 2.10, p. 172 in [3].

The system (4) has critical points at $(-2, 0)$ and $(1, 0)$; and for $-1 \ll \alpha < 0$ there is one limit cycle around $(-2, 0)$ and two limit cycles around $(1, 0)$; cf. [11], p. 170. The variation of these limit cycles with α can be studied analytically using Duff's theory for limit cycles of rotated vector fields; cf. [5]. However, in order to apply this theory to show that the two limit cycles around $(1, 0)$ intersect in a semistable limit cycle which

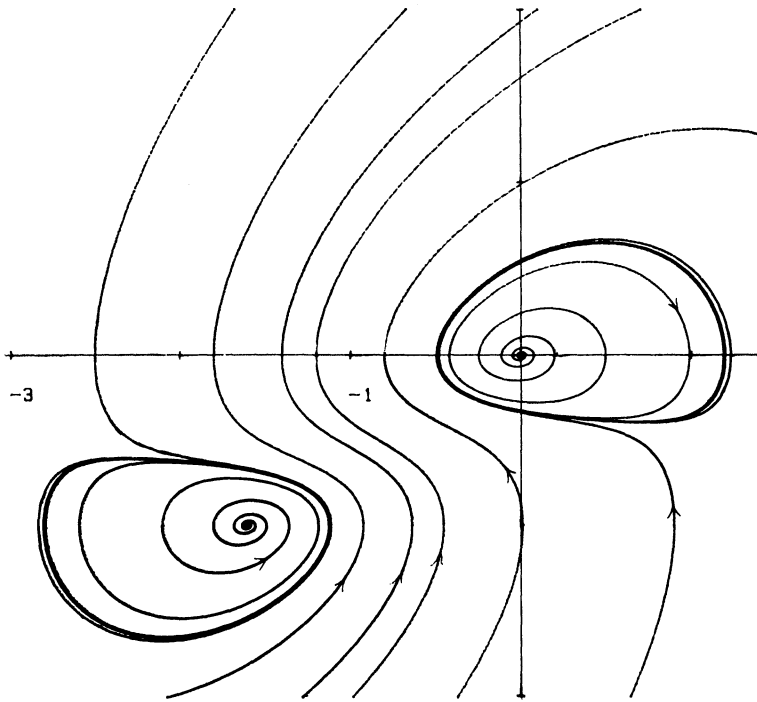


Figure 5

disappears as α decreases, it is necessary to assume that no other semistable limit cycles appear around the critical point $(1, 0)$. Since a semistable limit cycle can be made to split into two limit cycles with a proper variation of α , cf. Theorem 8, p. 23 in [5], this is equivalent to assuming that there are at most three limit cycles around the critical point $(1, 0)$. This seems like a reasonable assumption in view of Bautin's result [2] that at most three limit cycles can disappear into a critical point of focus or center type for a quadratic system and since there is no known example of a quadratic system with more than three limit cycles around a single critical point. Under the assumption that there are at most three limit cycles around the critical point $(1, 0)$, the following theorem can be proved. This theorem, together with the phase portraits in Figure 6 below, describes the global behavior of the limit cycles of the system (4) as α varies in $[-\pi, \pi]$; i.e., as the vector field goes through one complete rotation.

THEOREM. *The quadratic system (4) forms a complete family of rotated vector fields with parameter $\alpha \in [-\pi, \pi)$. A unique, negatively-oriented*

limit cycle, L_1 , is generated at the critical point $(1, 0)$ at $\alpha = 0$. Under the assumption that there are at most three limit cycles around the critical point $(1, 0)$, it follows that there exists a unique $\alpha^* \in (-\pi/2, 0)$ such that for all $\alpha \in (\alpha^*, 0)$, there is a second, negatively-oriented limit cycle, L_2 , around $(1, 0)$. The limit cycle L_1 is unstable and expands monotonically as α decreases in the interval $(\alpha^*, 0)$, and the limit cycle L_2 is stable and contracts monotonically as α decreases in the interval $(\alpha^*, 0)$. The two limit cycles intersect in a negatively-oriented semistable limit cycle, stable on its exterior and unstable on its interior, at $\alpha = \alpha^*$. This semistable limit cycle disappears as α is decreased below the critical value α^* .

PROOF. As is pointed out in [5], p. 16, the system (4) is an example of a complete family of rotated vector fields where the vectors are of constant length for $-\pi \leq \alpha < \pi$. Translating the origin of (4) to the critical point $(1, 0)$ leads to the system

$$\dot{x} = x \sin \alpha + y \cos \alpha + \frac{1}{3}x^2 \sin \alpha + xy(\cos \alpha - \frac{1}{3} \sin \alpha) - \frac{1}{2}y^2 \sin \alpha$$

$$\dot{y} = -x \cos \alpha + y \sin \alpha - \frac{1}{3}x^2 \cos \alpha + xy(\sin \alpha + \frac{1}{3} \cos \alpha) + \frac{1}{2}y^2 \cos \alpha.$$

This system has an elementary critical point at the origin with determinant $\Delta(\alpha) = 1$ and trace $\tau(\alpha) = 2 \sin \alpha$. It follows that at $\alpha = 0$ the origin is a weak focus. And it follows from the conditions given in Theorem 4.1, p. 175 of [3], which are necessary and sufficient for a quadratic system to have a center, that the origin of the above system is not a center for $\alpha = 0$. It therefore follows from the theory of rotated vector fields, cf. Theorem 10 in [5], that a unique limit cycle is generated at the critical point $(1, 0)$ of (4) at $\alpha = 0$. Since for $\alpha \in (-\pi/2, \pi/2)$ the flow is downward across the positive x -axis of the above system, this limit cycle is negatively oriented. Also since the x -axis consists of trajectories for $\alpha = \pm \pi/2$, there can be no limit cycle around the origin of the above system for $\alpha = \pm \pi/2$.

Tung Chin-chu [11] showed that there exists an $\alpha_0 < 0$ such that for all $\alpha \in (\alpha_0, 0)$ there are two negatively-oriented limit cycles, L and L_2 , around the critical point $(1, 0)$ of (4) with $L \subset \text{Int}(L_2)$, and with L unstable and L_2 stable. The critical point $(1, 0)$ is stable for $\alpha \in (-\pi/2, 0)$. Under the assumption that there are at most three limit cycles around $(1, 0)$, it follows from the Poincaré-Bendixson Theorem that if a third limit cycle occurs in $\text{Int}(L)$ or in $\text{Int}(L_2) \cap \text{Ext}(L)$, it must be a semistable limit cycle. But according to the theory of rotated vector fields, cf. Theorem 8 in [5], under a suitable small variation of α , a semistable limit cycle can be made to split into two limit cycles. This would result in four limit cycles around $(1, 0)$, contradicting the assumption that there are at most three limit cycles around $(1, 0)$. Thus, under the hypotheses of this theo-

rem, no limit cycles appear in $\text{Int}(L)$ or in $\text{Int}(L_2) \cap \text{Ext}(L)$. It then follows from the theory of rotated vector fields, cf. Theorems 7 and 9 in [5], that L is the limit cycle generated at the critical point $(1, 0)$ at $\alpha = 0$; i.e., $L = L_1$. And it follows from Theorem 7 and Table I on p. 21 of [5], which is reproduced in the introduction of this paper, that L_1 expands monotonically as α decreases and that L_2 contracts monotonically as α decreases. And then according to the theory of rotated vector fields outlined in the introduction, cf. Theorem *D* and the corollary to Theorem *G* in [7], as the parameter α varies monotonically, any limit cycle $L(\alpha)$ of (4) covers an annular neighborhood of its initial position and the inner and outer boundaries of this region consist of either a single critical point, a separatrix cycle on the Poincaré Sphere, or a semistable limit cycle. It therefore follows, by repeating the above argument to show that there are no limit cycles in $\text{Int}(L_2) \cap \text{Ext}(L_1)$, that as α decreases monotonically from zero, the unstable limit cycle L_1 , generated at the critical point $(1, 0)$ at $\alpha = 0$, expands monotonically from the point $(1, 0)$ until it intersects the contracting stable limit cycle L_2 at some critical value of α , $\alpha^* \in (-\pi/2, 0)$, thereby forming a semistable limit cycle unstable on its interior and stable on its exterior. And it follows from the theory of rotated vector fields, cf. Theorem 8 in [5], that as α decreases below α^* , this semistable limit cycle disappears. This completes the proof of the theorem.

The critical value α^* referred to in the above theorem has been shown to be approximately equal to $-.0093$; cf. Figure 11 below. Also, the limit cycle L_2 referred to in the above theorem expands to infinity as α increases to zero; cf. Figure 6 below. This follows from the theory of rotated vector fields, cf. Theorem 9 in [5] or the corollary to Theorem *G* in [7], and the fact that the flow is to the right across the y -axis for $\alpha^* < \alpha < 0$.

In order to determine the global behavior of Tung's system (4) for $\alpha \in [-\pi, \pi)$, it is necessary to determine the nature of the critical points at infinity for that system. R.W. Packard of the Department of Mathematics at Northern Arizona University and I have shown that the system (4) has exactly two critical points at infinity for all $\alpha \in [-\pi, \pi]$; cf. Lemma 10 in [11] which establishes this result for $|\alpha| \ll 1$. We have also numerically established that the determinant $\Delta(\alpha, k(\alpha))$, defined by eq. (11) on p. 160 of [11] with $k(\alpha)$ the real root of the cubic eq. $f(\alpha, k) = 0$, defined by eq. (7) on p. 159 of [11], is negative for all $\alpha \in [-\pi, \pi]$. (We have shown that $\Delta(\alpha, k(\alpha))$ has a negative maximum on $[-\pi, \pi]$.) And this implies that the two critical points at infinity of the system (4) are saddles for all $\alpha \in [-\pi, \pi]$. Furthermore, it follows from the theory of rotated vector fields, cf. Theorem 10 in [5] or the corollary to Theorem *H* in [7],

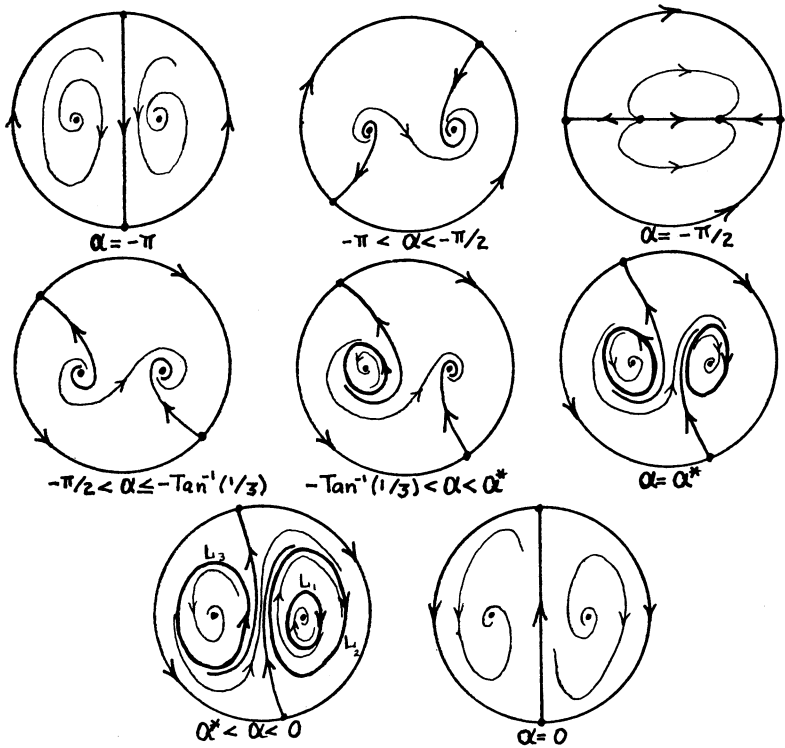


Figure 6

that a unique limit cycle, L_3 , is generated at the critical point $(-2, 0)$ at $\alpha = -\text{Tan}^{-1}(1/3)$. And then, under the assumption that this limit cycle is unique and that there are at most three limit cycles around $(1, 0)$, it follows from the Poincaré-Bendixson Theorem and the theory of rotated vector fields that the global phase portrait for the system (4) undergoes the continuous deformation depicted in Figure 6 as α varies in $[-\pi, 0]$. The global phase portrait for $\alpha \in [0, \pi]$ is obtained simply by reversing the arrows in the corresponding phase portrait in Figure 6 with $\alpha - \pi \in [-\pi, 0]$. Note that the limit cycle configuration (e) in Figure 1 is obtained for any $\alpha \in (\alpha^*, 0)$ where $\alpha^* \cong -.0093$.

A numerical plot showing two trajectories of the system (4) with $\alpha = -.1$ is shown in Figure 7 below. This figure illustrates the fifth configuration in Figure 6 with one unstable limit cycle around $(-2, 0)$.

The limit cycle L_3 around $(-2, 0)$ expands monotonically to infinity as α increases from $-\text{Tan}^{-1}(1/3)$ to 0. For $\alpha = -.009$ the limit cycle L_3 is shown in Figure 8 below. Actually, Figure 8 shows a single trajectory

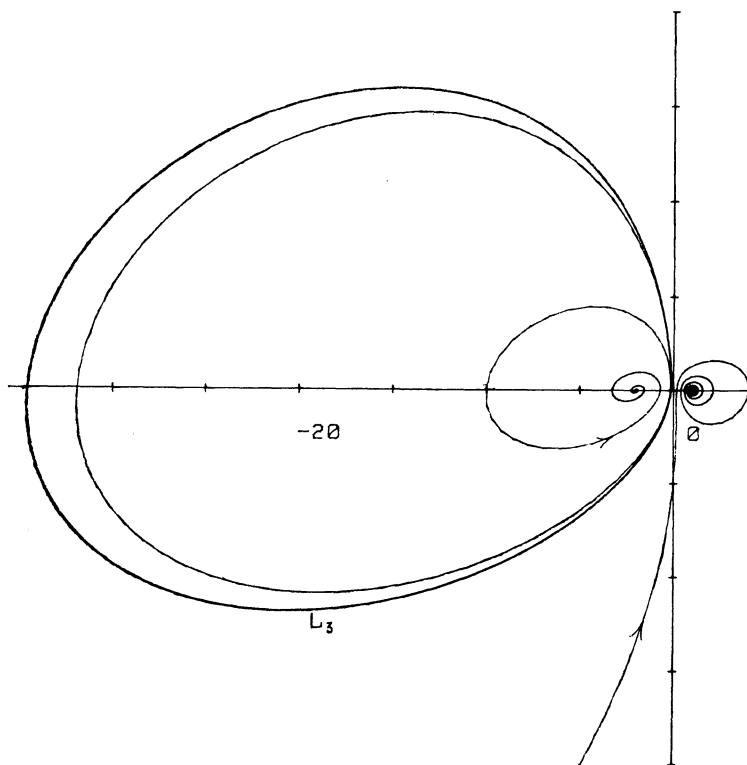


Figure 7

spiraling in from L_3 to the stable critical point $(-2, 0)$, but by computing the trajectory backward in time and letting the program run for a sufficiently long time, a computer plot of L_3 is obtained. Also for $\alpha = -.009$, the two limit cycles L_1 and L_2 around $(1, 0)$ are shown in Figure 9 below. Figures 8 and 9 then show the shapes and sizes of the three limit cycles in the configuration (e) for Tung Chin-chu's quadratic system (4) with $\alpha = -.009$.

As α varies in $(-\tan^{-1}(1/3), 0)$, the growth of the limit cycle, L_3 , around $(-2, 0)$ is described in Figure 10; and as α varies in $(\alpha^*, 0)$, the growth of the two limit cycles, L_1 and L_2 , around $(1, 0)$ is described in Figure 11 which also shows that $\alpha^* \cong -.0093$.

The inverse of each of the relationships shown in Figures 10 and 11 describes a continuous function, $\alpha(x)$, defined on $[0, \infty)$. This is the function described in Theorem 3, p. 340 in [15] for a general class of quadratic systems. And Figures 10 and 11 below correspond to the first and second graphs shown in Figure 4, p. 340 in [15] respectively.

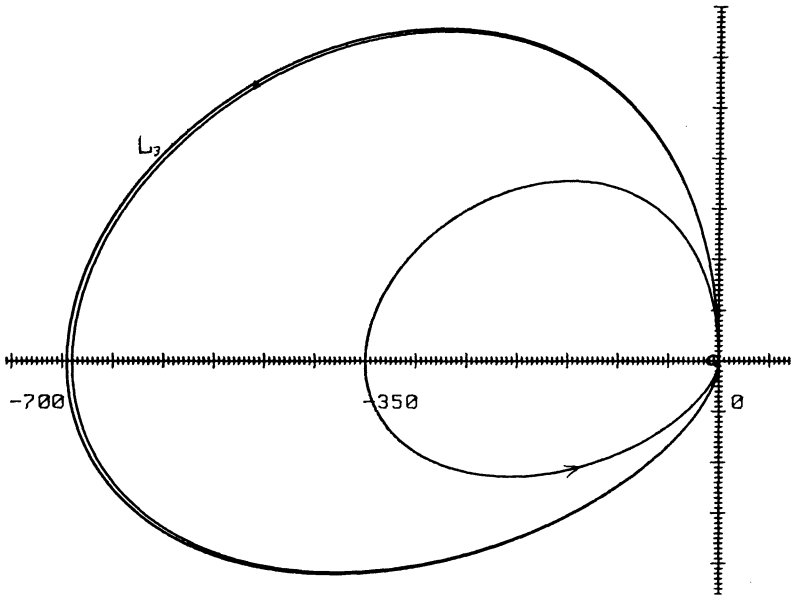


Figure 8

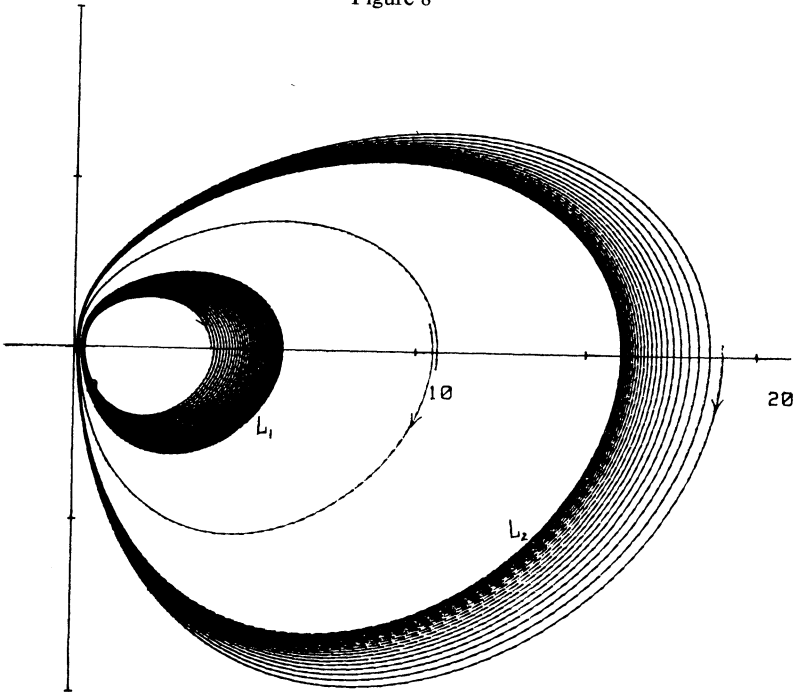


Figure 9

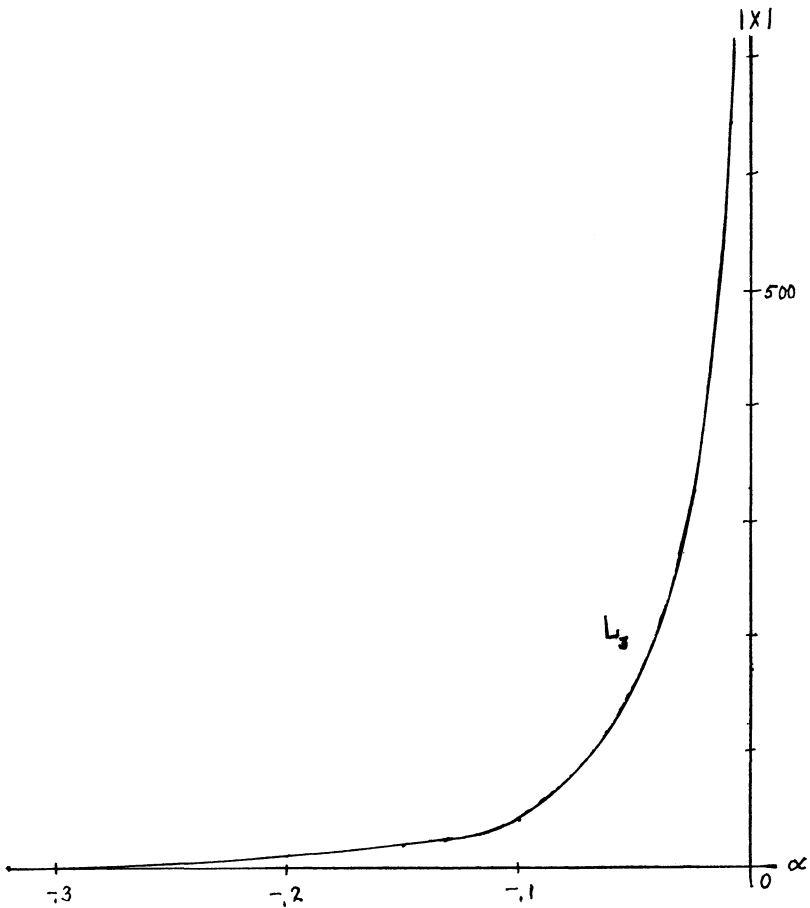


Figure 10

4. Songling's example of the configuration (f). It was recently established in [10] that the quadratic system

$$(5) \quad \begin{aligned} \dot{x} &= P(x, y) \equiv \lambda x - y - 10x^2 + (5 + \delta)xy + y^2 \\ \dot{y} &= Q(x, y) \equiv x + x^2 + (8\varepsilon - 25 - 9\delta)xy \end{aligned}$$

with $\lambda = -10^{-200}$, $\varepsilon = -10^{-52}$, and $\delta = -10^{-13}$ has at least four limit cycles in the configuration (f). It is still an open problem to determine whether or not this system has exactly four limit cycles in the configuration (f). Songling also established that the system (5) has the separatrix

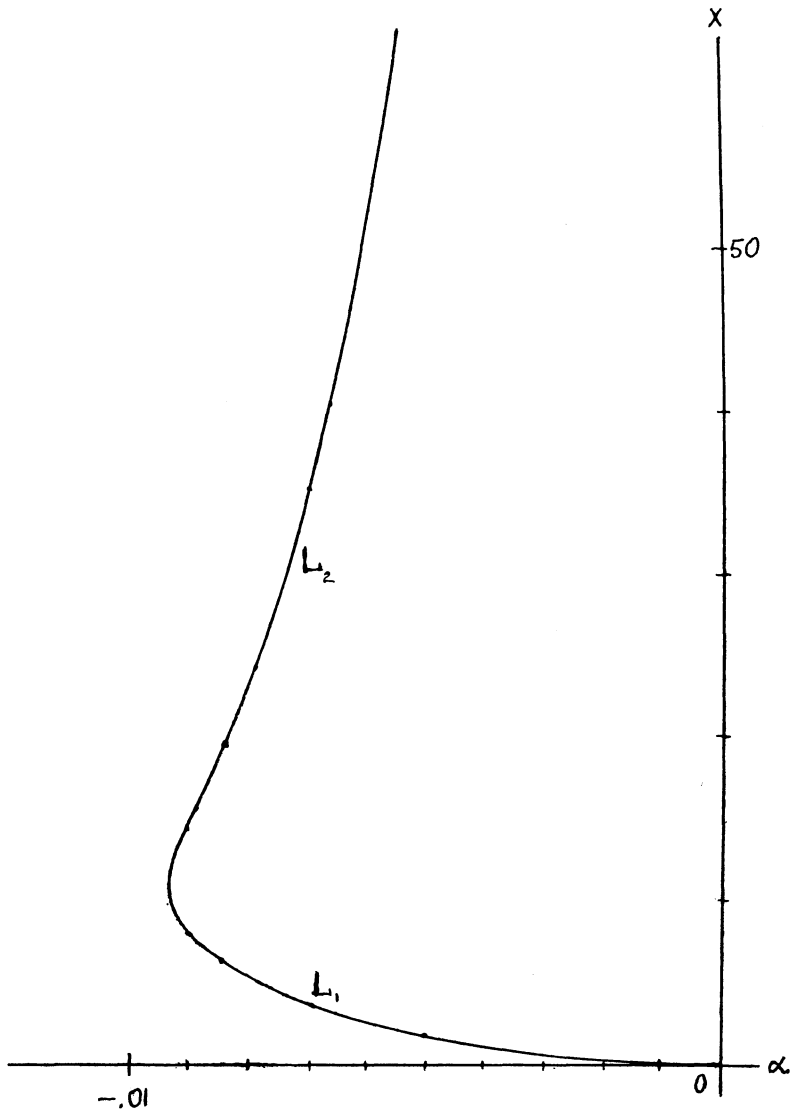


Figure 11

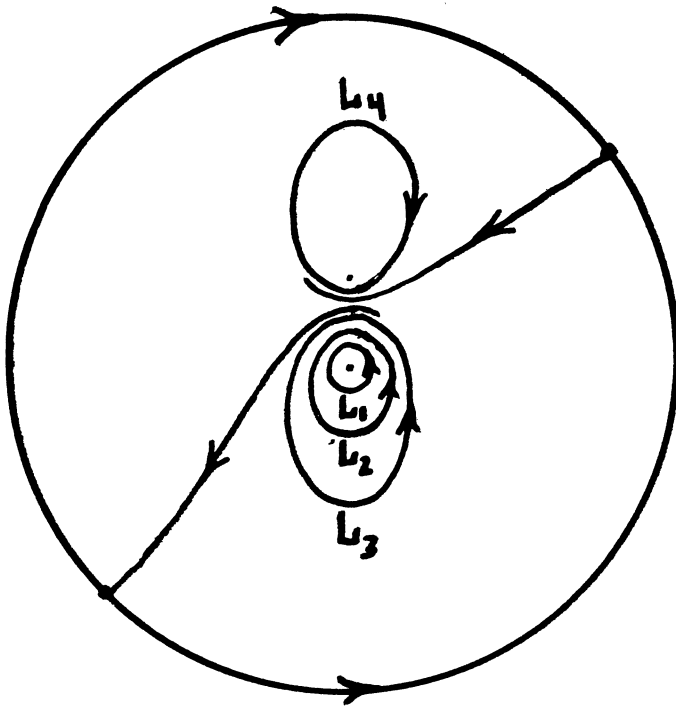


Figure 12

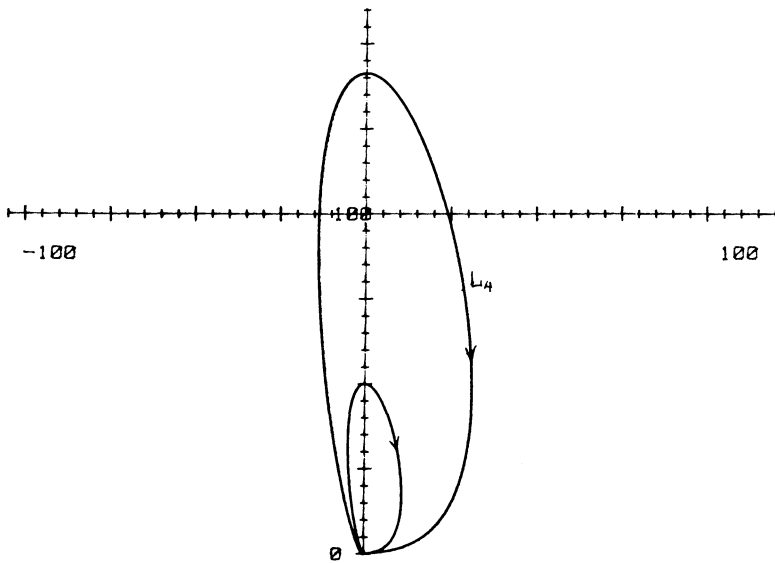


Figure 13

configuration shown in Figure 12 above with critical points at $(0, 0)$ and $(0, 1)$; cf. [10] p. 158.

The limit cycle L_4 around $(1, 0)$ is very large in comparison to the three limit cycles around the origin. It is very easy to plot this limit cycle numerically since all trajectories starting on the segment $1 < y < \infty$ spiral in or out to L_4 very rapidly. Figure 13 above shows a single trajectory spiraling out from $(0, 1)$ to L_4 . The outer curve, to within the pen-width, is the limit cycle L_4 .

Figure 14 below shows the general configuration of trajectories near the two finite critical points at $(0, 0)$ and $(1, 0)$. It appears that there is a trajectory spiraling out from the unstable limit cycle L_3 around the origin and that L_3 intersects the negative y -axis at $y_3 \cong -.4$. This, however, is not the case as a study of the Poincaré return map clearly shows.

The Poincaré return map on a ray from the origin can be defined by writing the system (5) in polar coordinates (r, θ) as

$$(5') \quad \frac{dr}{d\theta} = F(r, \theta) \equiv r \left[\frac{xP(x, y) + yQ(x, y)}{xQ(x, y) - yP(x, y)} \right]$$

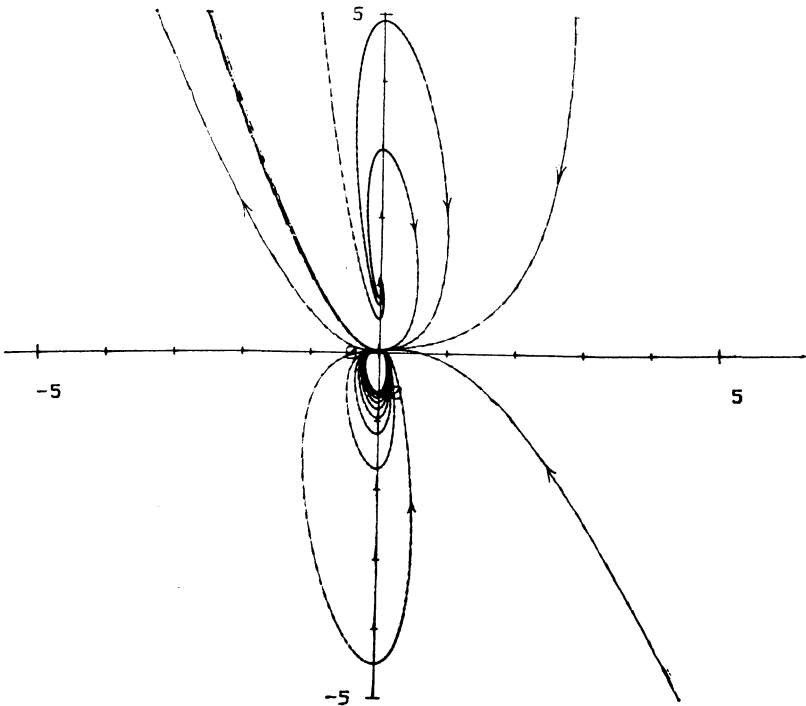


Figure 14

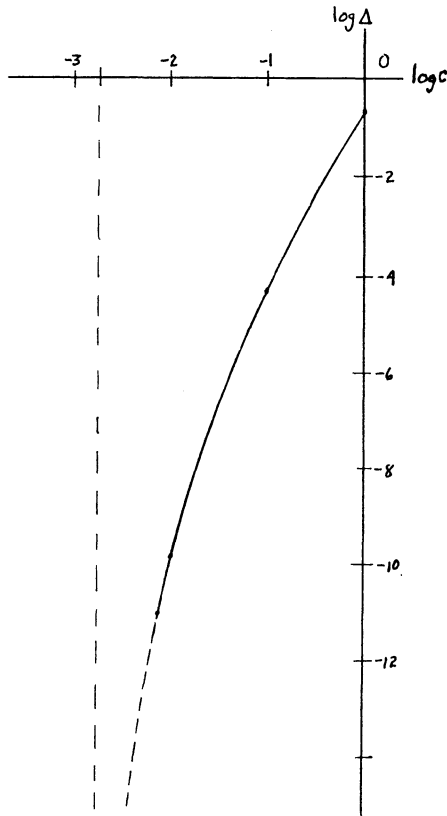


Figure 15

with $x = r \cos \theta$ and $y = r \sin \theta$, and P and Q defined by (5). We then compute the change in $r(\theta)$ as θ changes by 2π . In view of the trajectory configuration in Figure 14, we compute this change along the negative y -axis; i.e., we compute $\Delta(c) = r(3\pi/2, c) - c$ where $c = r(-\pi/2)$.

Figure 15 shows $\Delta(c)$ on a log-log scale. It indicates that the limit cycle L_3 intersects the negative y -axis at a value y_3 with $10^{-3} < |y_3| < 10^{-2}$; however, even carrying 16 figures and using an extremely small step size in the fourth order Runge-Kutta integration scheme, $h = .0001$, it was only possible to obtain eleven figure accuracy in Δ due to round-off error. And the computation of $\Delta(c)$ could only be carried down to $c \cong .008$ since $|\Delta(c)| < 10^{-11}$ for all $c < .008$. Thus, the size of L_2 and L_1 cannot be determined by this method. All that is known at this time is that $10^{-61} < |y_2| < 10^{-19}$ and that $0 < |y_1| < 10^{-60}$; this was established by Songling in [10], pp. 155-156.

5. A Modification of Songling's Example. In order to obtain a quadratic system with four limit cycles of "normal size" in the configuration (f), Songling's example was modified as follows. The system (5) was first embedded in a uniformly rotated vector field; cf. [5], p. 16:

$$(6) \quad \begin{aligned} \dot{x} &= P(x, y) \cos \alpha - Q(x, y) \sin \alpha \\ \dot{y} &= P(x, y) \sin \alpha + Q(x, y) \cos \alpha \end{aligned}$$

with P and Q defined in (5). Then according to the theory of rotated vector fields, cf. [5], p. 21, the positively oriented, unstable limit cycle L_3 expands as α increases. For example, for $\alpha = .001$ in (6) the unstable limit cycle L_3 with $|y_3| \cong .5$ shown in Figure 16 below was obtained.

The variation of the size of L_3 with α as well as the qualitative behavior of L_1 and L_2 with α is shown in Figure 17 where y_L denotes the intersection

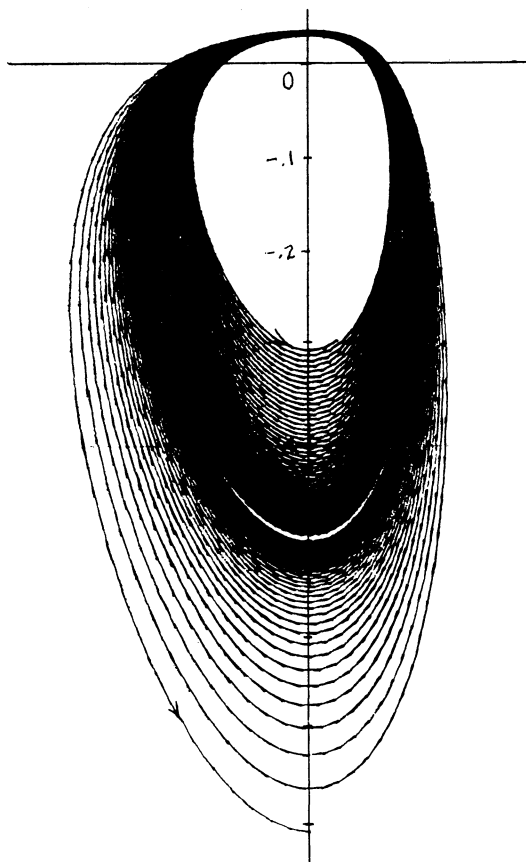


Figure 16

of the limit cycle with the negative y -axis. The dashed curve indicates the qualitative behavior of the limit cycles $L_1(\alpha)$, $L_2(\alpha)$, and $L_3(\alpha)$ around the origin of (6) which follows from Songling's results [10] and the theory of rotated vector fields [5, 7] under the assumption that there are at most three limit cycles around the origin. In particular, it follows from the corollary to Theorem H in [7] that the limit cycle L_1 is generated at the origin at that value of α for which the trace of the linear part of (6) is zero; i.e., at $\alpha = \tan^{-1}(\lambda/2)$.

Once an ordinary-size limit cycle that can be seen with the aid of the computer is obtained, the effect of varying the coefficients λ , ϵ , and δ in the system (6) on the limit cycles L_1 , L_2 and L_3 can be determined. Without going into detail, it was determined that increasing the parameter δ in (5) increased the size of L_3 and that λ and ϵ determined the size of L_1 and L_2 . For $\lambda = -.005$, $\epsilon = -.01$, and $\delta = -.5$, in (5), the limit cycles L_1 , L_2

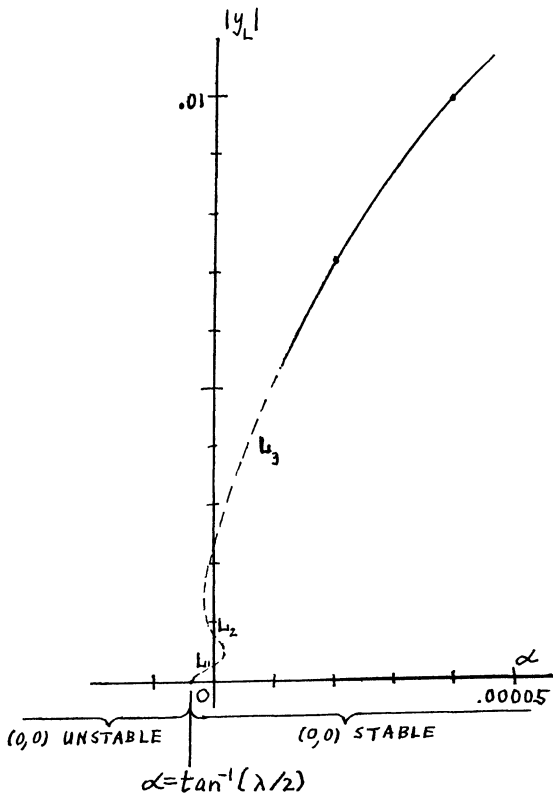


Figure 17

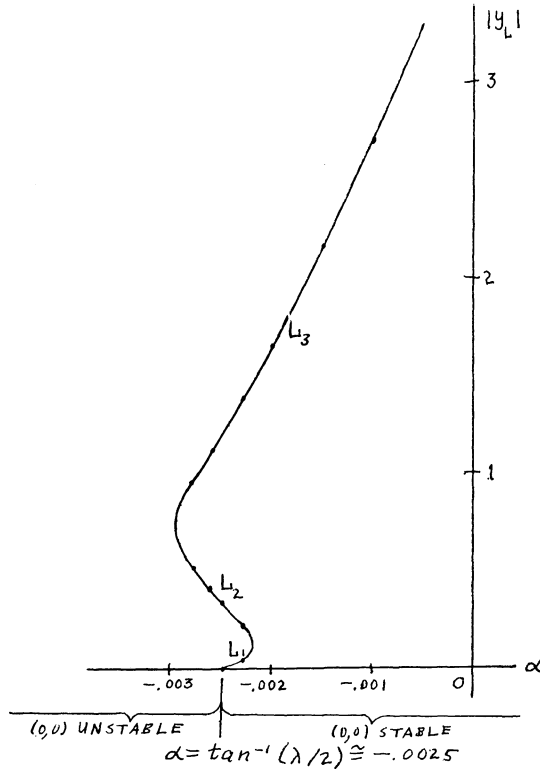


Figure 18

and L_3 around the origin of the system (6) varied with α as described in Figure 18 above.

The inverse of the relationship shown in Figure 18 describes a continuous function, $\alpha(y)$, defined on $[0, \infty)$. This is the function described in Theorem 3, p. 340 in [15] and Figure 18 corresponds to the third graph shown in Figure 4, p. 340 in [15].

In particular, for $\alpha = -0.0023$, there are three limit cycles around the origin. The quantity $\Delta(c)/c$, defined in §3, which describes the Poincaré map along the negative y -axis is shown in Figure 19 below.

Figure 19 clearly shows that there are exactly three limit cycles around the origin of (6). Furthermore, the computational results used in drawing this figure also determine the values of $y_1 = -0.0425$, $y_2 = -0.2160$, and $y_3 = -1.3838$ to four figure accuracy. Using these values as initial conditions, a plot of the limit cycles L_1 , L_2 and L_3 was obtained. These three

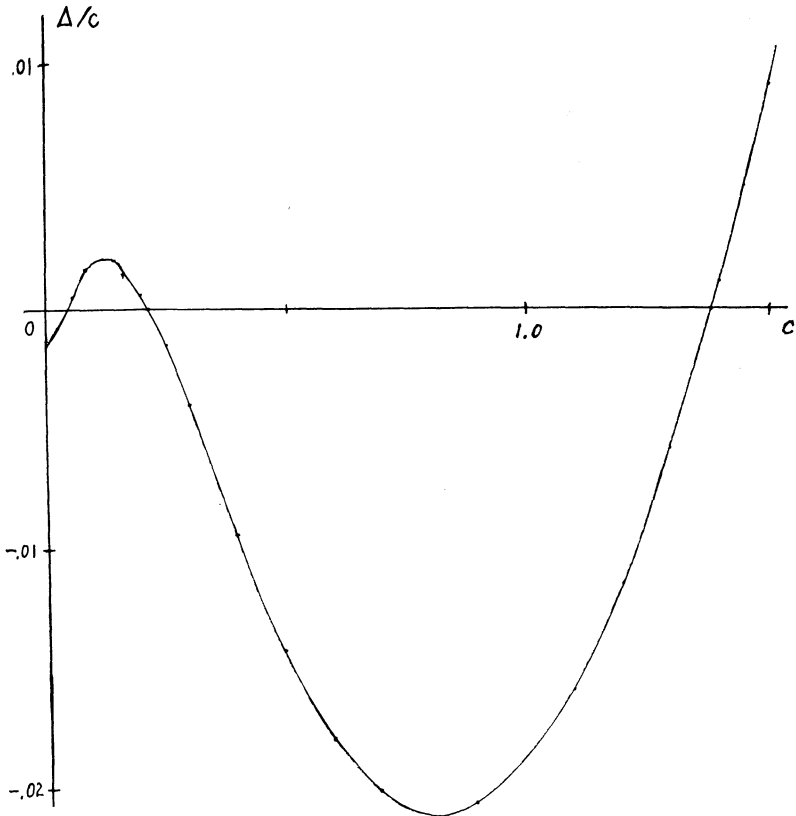


Figure 19

limit cycles and a piece of the limit cycle L_4 are shown in Figure 20 below. The entire limit cycle L_4 is shown in Figure 21. Figures 20 and 21 then show the four limit cycles of the system (6) with $\delta = -.5$, $\varepsilon = -.01$, $\lambda = -.005$, and $\alpha = -.0023$ in the configuration (f) of Figure 1.

6. Chin's Examples of the Configurations (b) and (c).

Bautin [2], pp. 18–19, showed that there exist quadratic systems with two and three limit cycles in a small neighborhood of the origin. Chin et al. [4] showed that for $\lambda = 10^{-820}$, $\delta = -10^{-350}$ and $\varepsilon = -10^{-78}$, the quadratic system

$$(7) \quad \begin{aligned} \dot{x} &= \lambda x - y + (2 + \delta)xy - y^2 \\ \dot{y} &= x + \lambda y + x^2 - (5 + \varepsilon)xy - y^2 \end{aligned}$$

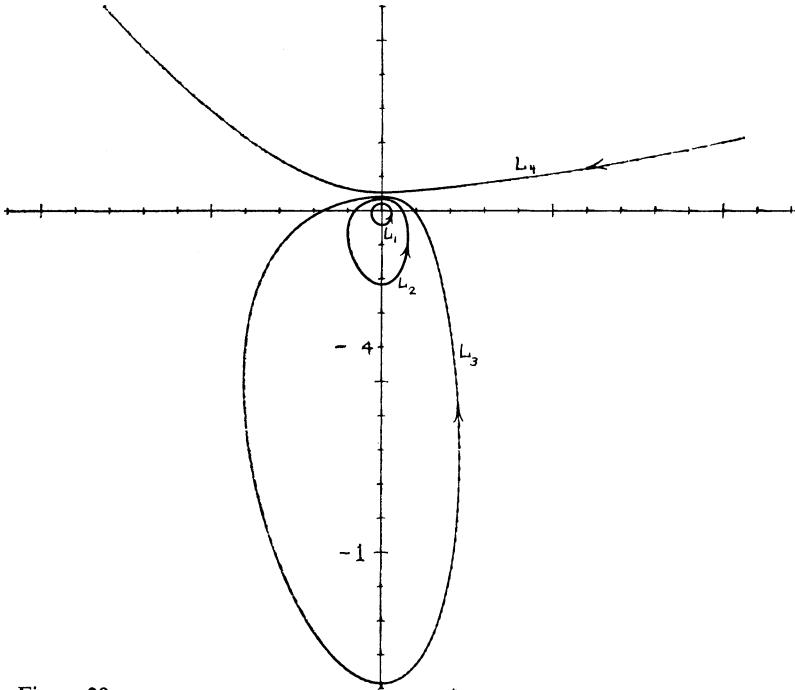


Figure 20

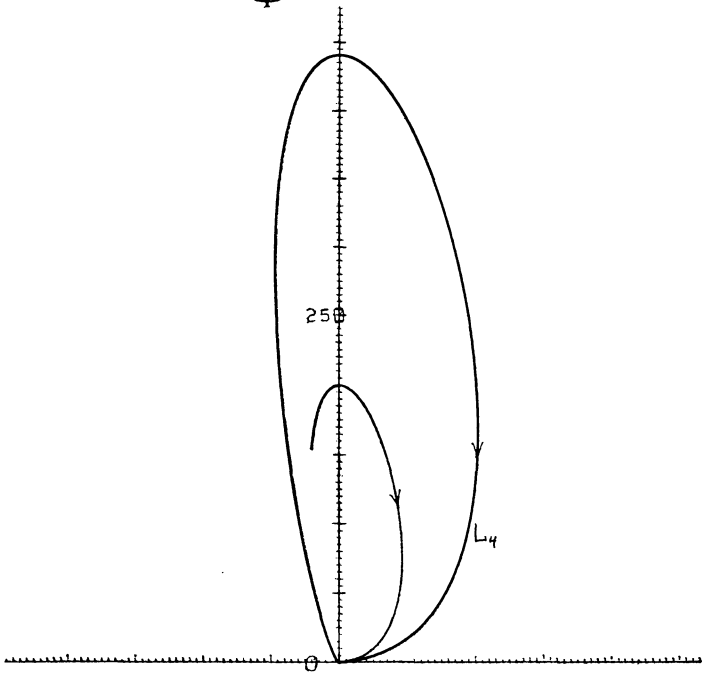


Figure 21

has three limit cycles around the origin in the configuration (c) of Figure 1 and that, by embedding the vector field (7) in a rotated family of vector fields, the configuration (b) in Figure 1 can be obtained for an appropriate rotation of the vector field.

Using Theorems 65 and 66 in [1], it can be shown that, under the assumption that there are at most three limit cycles around the origin, the separatrix configuration for (7) is given by the configuration in Figure 22.

The configuration of trajectories near the four finite critical points of the system (7) is shown in Figure 23.

The limit cycles around the origin of (7) are extremely small, too small in fact to be determined by the numerical methods used in this paper. By embedding (7) in a family of rotated vector fields as in (6), the size of the largest limit cycle around the origin, which is a positively-oriented, stable limit cycle, can be increased by decreasing α from 0. For example, for $\alpha = -.001$ a limit cycle just inside the inner curve around the origin in Figure 23 is obtained. It also follows by embedding (7) in a family of rotated vector fields and using Duff's Theorem 10 and his estimate for the growth of a limit cycle with α , eq. (3.17), p. 23, in [5], that the smallest

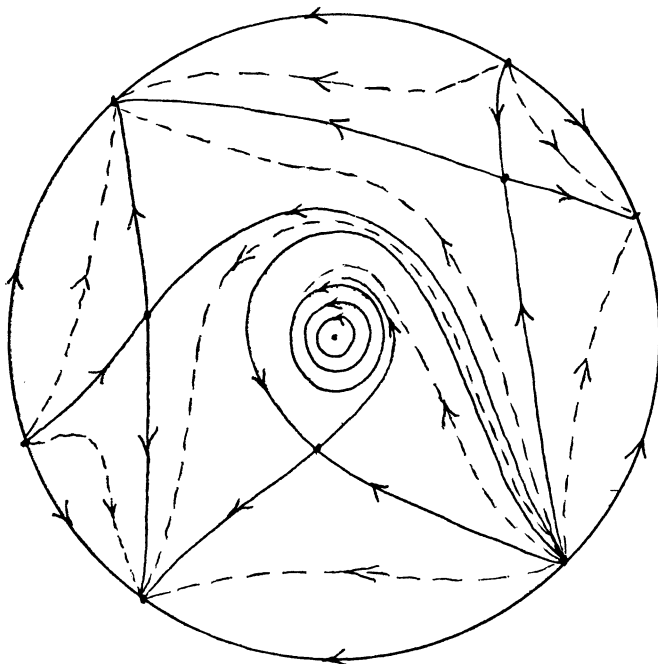


Figure 22

limit cycle in Chin's example (7) is very nearly a circle with a diameter of $0(10^{-820})$.

It follows from Chin's results [4] and the theory of rotated vector fields [5] that, under the assumption that there are at most three limit cycles around the origin, the same qualitative behavior of the three limit cycles of the system (6) with P and Q given by (7) is obtained as is depicted in Figure 17, only with $\alpha \rightarrow -\alpha$ since Chin's limit cycles have the opposite stability of Songling's limit cycles.

Mieussens [14] has shown numerically that Chin's system (7) with $\varepsilon = .1$, $\delta = -.06$, and $\lambda = -.0001$ has two limit cycles in the configuration (b) of Figure 1. He also shows that the larger limit cycle, L_2 , intersects the positive x -axis at $x_2 \cong .213$; he does not locate the smaller limit cycle L_1 , but only states that L_1 intersects the positive x -axis in a neighborhood of the point $(.1, 0)$.

By studying the Poincaré map along the negative y -axis, i.e., by computing the quantity $\Delta(c)$ defined in §3, for Mieussens modification of Chin's example, it is possible to approximate the initial conditions for both of the limit cycles L_1 and L_2 . The quantity $\Delta(c)/c$ is shown in Figure

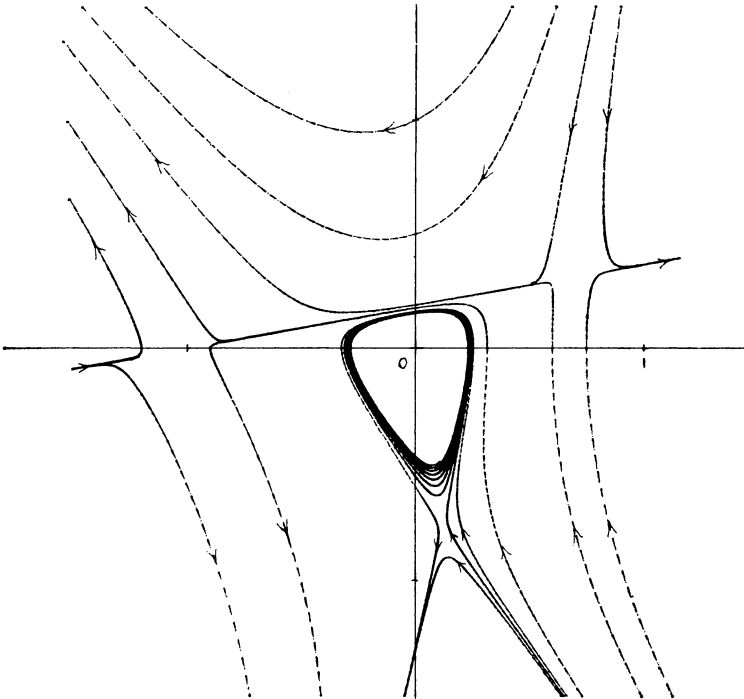


Figure 23

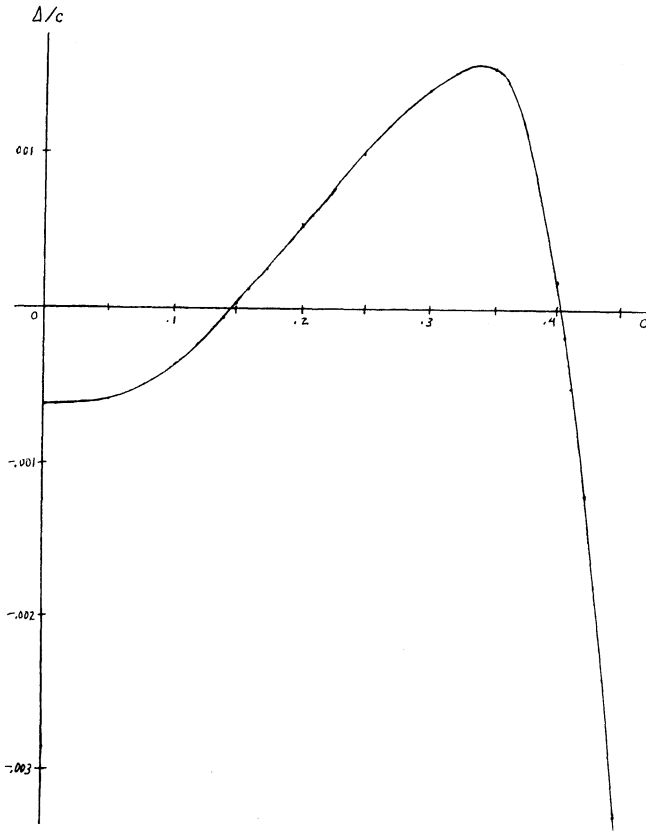


Figure 24

24 and it follows that $y_1 \cong -.146$ and $y_2 \cong -.403$. Using these values as initial conditions, plots of the limit cycles L_1 and L_2 in the configuration (b) of Figure 1 were obtained. These limit cycles are shown in Figure 25 below.

A modification of Chin's example with three normal-size limit cycles in the configuration (c) of Figure 1 has not yet been obtained.

7. Closing Remarks. This completes this numerical study of the known limit cycle configurations of quadratic systems in the plane. Two important mathematical problems are suggested by this study.

1. Determine the exact number of limit cycles in the examples of Songling [10] and Tung Chin-chu [11], a problem previously suggested by Chicone and Jinghuang [3].

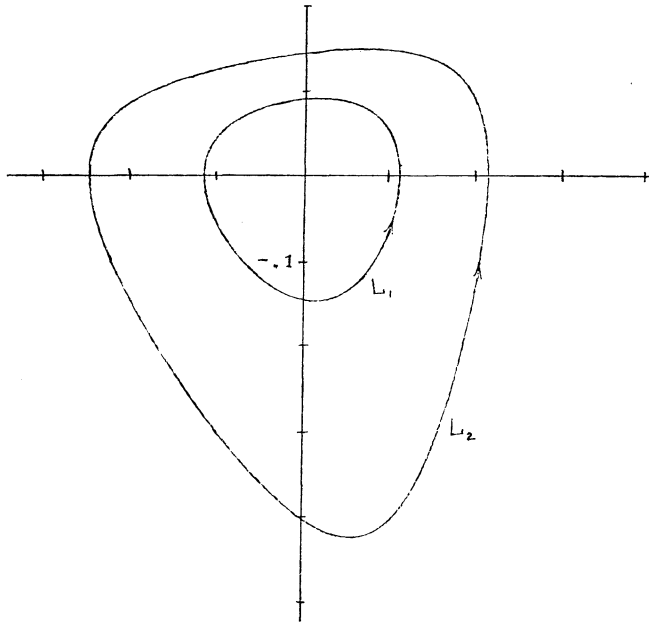


Figure 25

2. Determine whether or not a quadratic system can have more than three limit cycles around a single critical point.

The second problem would have a direct bearing on Hilbert's problem 16 for quadratic systems. In fact, if a quadratic system can have at most three limit cycles around any one critical point, it would then follow from Theorem 2.9(c) in [3] that the maximum number of limit cycles possible for a quadratic system is less than or equal to six. It follows from Songling's example that this number is greater than or equal to four.

All of the plots in this paper were drawn on a HP 9845 desk-top computer. A fourth order Runge Kutta method with a variable step size was used to solve the initial value problem associated with the system (1).

The author wishes to thank Prof. Robert Packard of the Department of Mathematics at Northern Arizona University for his help in computing the determinant that occurs in Tung Chin-chu's example, and to thank Paul Davidson, a graduate student in the Department of Mathematics and Physics, for his help in computing the values of the Poincaré maps used in this paper.

REFERENCES

1. A.A. Andronov et al., *Qualitative Theory of Second-Order Dynamical Systems*, John Wiley and Sons, N.Y. 1973.
2. N.N. Bautin, *On the number of limit cycles which appear with a variation of coefficients from equilibrium position of focus or center type*, Mat. Sb., **30** (1952), 181–196; Am. Math. Soc. Transl., No. **100** (1954), 3–19.
3. C. Chicone and Tian Jinghuang, *On general properties of quadratic systems*, Am. Math. Monthly, **89** (1982), 167–178.
4. Chin Yuan-Shun et al., *Concrete examples of the existence of three limit cycles for the system $dx/dt = X_2(x, y)$, $dy/dt = Y_2(x, y)$* , Acta Math. Sinica, **9** (1959), 213–226.
5. G.D.F. Duff, *Limit cycles and rotated vector fields*, Annals of Math., **67** (1953), 15–31.
6. M. Frommer, *Über das Auftreten von Wirbeln und Strudeln in geschlossener und spiralförmiger Integralkurven in der Umgebung rationaler Unbestimmtheitsstellen*, Math. Ann., **109** (1934), 395–424.
7. L.M. Perko, *Rotated vector fields and the global behavior of limit cycles for a class of quadratic systems in the plane*, J. Diff. Eq., **18** (1975), 63–86.
8. L.M. Perko and Shu Shih-lung, *Existence, uniqueness, and non-existence of limit cycles for a class of quadratic systems in the plane*, J. Diff. Eq. **53** (1984), 1–26.
9. I.G. Petrovskii and E.M. Landis, *On the number of limit cycles of the equation $dy/dx = P(x, y)/Q(x, y)$ where P and Q are polynomials of the second degree*, Mat. Sb., **37** (1955), 209–250; Am. Math. Soc. Transl., Ser. 2, **10** (1958), 177–221.
10. Shi Songling, *A concrete example of the existence of four limit cycles for plane quadratic systems*, Sci. Sinica, **23** (1980), 153–158.
11. Tung Chin-chu, *Positions of limit cycles of the system $dx/dt = \sum a_{ik}x^i y^k$, $dy/dt = \sum b_{ik}x^i y^k$, $0 \leq i + k \leq 2$* , Sci. Sinica, **8** (1959), 151–171.
12. Yeh Yen-chien, *Periodic solutions and limit cycles of certain nonlinear differential systems*, Sci. Record N.S., **1** (1957), 391–394.
13. ———, *A qualitative study of the integral curves of the differential equation $dy/dx = \dots$, I, Uniqueness of limit cycles II*, Chinese Math., 1–18 (1963), 62–70.
14. Mieussens, M., *Sur les cycles limites de $dy/dx = -[x + (1 + \varepsilon)x^2 + 2xy - y^2]/[y - 2xy + y^2]$ et $dy/dx = [x + \lambda y + x^2 - (5 + \varepsilon)xy - y^2]/[\lambda x - y + (2 + \delta)xy - y^2]$* , CNRS Report No. 7803, Université de Bordeaux, 1978.
15. ———, *Sur les cycles limites des systèmes quadratiques*, C.R. Acad. Sci. Paris, **291** Série A (1980), 337–340.

NORTHERN ARIZONA UNIVERSITY, FLAGSTAFF, AZ 86011

